

Kinetic Mechanism of the Inhibition of Cathepsin G by α_1 -Antichymotrypsin and α_1 -Proteinase Inhibitor

Jérôme Duranton, Christophe Adam, and Joseph G. Bieth*

Laboratoire d'Enzymologie, INSERM U 392, Université Louis Pasteur de Strasbourg, France

Received January 28, 1998; Revised Manuscript Received May 20, 1998

ABSTRACT: Uncontrolled proteolysis due to cathepsin G (cat G) may cause severe pathological disorders. Cat G is inhibited by α_1 -antichymotrypsin (ACT) and α_1 -proteinase inhibitor (α_1 PI), two members of the serpin superfamily of proteins. To see whether these two inhibitors play a physiological proteolysis-preventing function, we have made a detailed kinetic investigation of their reaction with cat G. The kinetics of inhibition of cat G in the presence of inhibitor and substrate evidenced a two-step inhibition

mechanism: $E + I \xrightleftharpoons{K_i^*} EI^* \xrightarrow{k_2} EI$. The cat G/ACT interaction is described by $K_i^* = 6.2 \times 10^{-8}$ M and $k_2 = 2.8 \times 10^{-2}$ s⁻¹, while the cat G/ α_1 PI association is governed by $K_i^* = 8.1 \times 10^{-7}$ M and $k_2 = 5.5 \times 10^{-2}$ s⁻¹. The reliability of these kinetic constants was checked using a number of experiments which all gave consistent results: (i) both EI^* complexes were found to be enzymatically inactive, (ii) the K_i^* values were determined directly using initial velocity experiments of cat G-catalyzed hydrolysis of substrate in the presence of inhibitor, (iii) the second-order rate constants k_2/K_i^* were measured using second-order inhibition experiments in the absence of substrate, and (iv) the ratio of the two second-order rate constants was determined by measuring the partition of cat G between the two fluorescently labeled serpins. Since the plasma concentrations of ACT and α_1 PI are much higher than their K_i^* values, cat G released from neutrophils will be fully taken up as rapidly forming EI^* complexes, that is, 70% with ACT and 30% with α_1 PI. Both ACT and α_1 PI are thus physiological cat G inhibitors whose inhibitory potential does not depend on the formation of the stable inhibitory species EI characteristic of serpins. Such an in vivo inhibition mechanism might take place with other serpin/proteinase systems.

The azurophil granules of neutrophils store a number of proteins that participate in phagocytosis. One of them, cathepsin G (cat G¹), is a cationic serine proteinase whose crystal structure has been determined recently (1). Its specificity is directed against substrates with a Phe or a Lys residue at the P₁ position (2). In vitro, cat G cleaves a number of extracellular matrix and plasma proteins including type II collagen, proteoglycans, elastin, fibronectin, laminin, fibrinogen, coagulation factors VIII and XII, immunoglobulins G and M, complement components (for a review see ref 3), angiotensinogen (4), and heparin cofactor (5). On the other hand, it is able to recruit, activate, and aggregate platelets (6). Uncontrolled release of cat G during phagocytosis or cell death may thus lead to matrix degradation, coagulation disorders, immunodeficiency, or vascular occlusion.

The aforementioned effects should normally be prevented by proteinase inhibitors present in plasma and tissues. These include ACT and α_1 PI, two members of the serpin family of inhibitors. The serpins have a highly conserved secondary structure comprising 9 α -helices and 3 β -sheets (7). They form denaturant-stable complexes with their target proteinases and behave kinetically like irreversible inhibitors (8,

9). The stable inhibitory complex is thought to be an acyl-enzyme formed between the carbonyl group of the serpin's P₁ residue and the hydroxyl group of the serine residue of the proteinase's active center (10, 11). ACT has a leucine residue at P₁ and is specific for chymotrypsin-like enzymes such as cat G, pancreatic chymotrypsin, mast cell chymase, and human pancreatic elastase (12–14). In contrast, α_1 PI, whose P₁ residue is methionine, inhibits proteinases with chymotrypsin-like, trypsin-like, and elastase-like specificities albeit with considerably different rates (8).

If a serpin inhibits a proteinase in one step ($E + I \rightarrow EI$) its in vivo efficiency is best defined by its delay time of inhibition, $d(t)$, that is, the time required to achieve full inhibition in vivo: $d(t) = 5/(k_{\text{assoc}}[I]_0)$ where k_{assoc} is the in vitro determined second-order association rate constant and $[I]_0$ is the in vivo serpin concentration. If $d(t) \leq 1$ s, the serpin is likely to prevent proteolysis in vivo (15). If a serpin inhibits a proteinase in more than one step, k_{assoc} will have a complex meaning so that the delay time of inhibition no longer predicts the in vivo inhibitor potency (16). The kinetic mechanism of inhibition must, therefore, be known to decide whether an inhibitor is physiologically relevant. This is the reason we have investigated the kinetic mechanism of inhibition of cat G by ACT and α_1 PI.

MATERIALS AND METHODS

Cat G was isolated and active-site titrated as described previously (17). ACT and α_1 PI were from Athens Research

* To whom correspondence should be sent at the following address: INSERM U 392, Faculté de Pharmacie, 74 route du Rhin, F-67400 Illkirch, France. Tel: 33 3 88 67 69 34. Fax: 33 3 88 67 92 42. E-mail: jgbieth@pharma.u-strasbg.fr.

¹ Abbreviations: cat G, cathepsin G; ACT, α_1 -antichymotrypsin; α_1 -PI, α_1 -proteinase inhibitor; Suc, succinyl; pNA, p-nitroanilide; SBZl, thiobenzyl ester.

Technology (Athens, GA) and were found to be electrophoretically pure. Molarities of inhibitor solutions were calculated using $\epsilon_{280\text{nm}} = 3.9 \times 10^4 \text{ M}^{-1} \text{ cm}^{-1}$ and $2.8 \times 10^4 \text{ M}^{-1} \text{ cm}^{-1}$ for ACT and $\alpha_1\text{PI}$, respectively (18). Suc-Ala₂-Pro-Phe-pNA and Suc-Ala₂-Pro-Phe-SBzl came from Bachem (Bubendorf, Switzerland), while 4,4-dithiodipyridine was from Sigma. Unless otherwise stated, all experiments were done at 25 °C in 50 mM Hepes and 150 mM NaCl, pH 7.4, a solution called "the buffer" throughout the text.

Enzymatic Methods. Titration of cat G with ACT and $\alpha_1\text{PI}$ was done by reacting constant concentrations of the enzyme (0.18 μM) with increasing concentrations of the serpins at pH 7.4 and 25 °C. After an incubation time of 15 min (ACT) or 30 min ($\alpha_1\text{PI}$), the residual enzymatic activities of the mixtures were determined with 2.5 mM Suc-Ala₂-Pro-Phe-pNA.

The kinetics of inhibition of cat G by the two serpins in the presence of substrate was assessed by adding enzyme to a mixture of inhibitor and substrate and continuously monitoring the release of product. Rapid mixing of the reagents was performed using a SFA-11 stopped-flow device (High-Tech, Salisbury, UK) connected to a computerized Uvikon spectrophotometer thermostated at 25 °C.

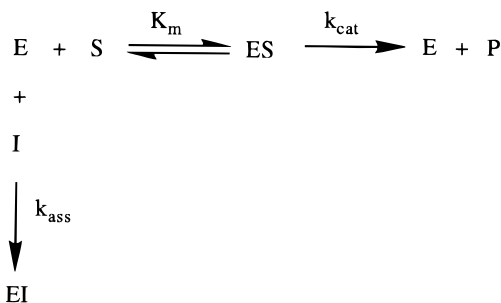
The second-order kinetics of inhibition of cat G by ACT and $\alpha_1\text{PI}$ was assessed by reacting equimolar concentrations of enzyme and inhibitor for variable periods of time before addition of the substrate Suc-Ala₂-Pro-Phe-SBzl.

All other conditions are given in the legends to the figures or in the text. Regression analyses of the data were done using the Enzfitter software from Biosoft.

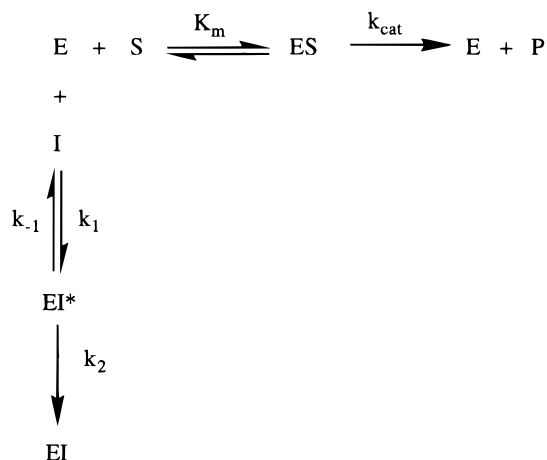
Fluorescent Labeling. One mole of ACT was reacted with 1.5 mol of fluorescein-5-EX, succinimidyl ester from Molecular Probes in 100 mM carbonate, pH 8.3. After 15 min of continuous stirring at room temperature, labeled ACT was isolated using a PD-10 gel filtration column (Amersham Pharmacia Biotech) equilibrated with the above buffer. There was 0.6 molecule of label/molecule of ACT as determined spectrophotometrically using $\epsilon_{495\text{nm}} = 92\,000 \text{ M}^{-1} \text{ cm}^{-1}$ for the protein-bound label. One mole of $\alpha_1\text{PI}$ was reacted with 2 mol of 6-(tetramethylrhodamine-5-(and-6)-carboxamido)hexanoic acid, succinimidyl ester from Molecular Probes in 50 mM TES and 150 mM NaCl, pH 7.0. After 1 h of continuous stirring at room temperature, labeled $\alpha_1\text{PI}$ was isolated using a PD-10 column equilibrated with the above buffer. There was 0.65 molecule of label/molecule of $\alpha_1\text{PI}$ as determined spectrophotometrically using $\epsilon_{560\text{nm}} = 77\,500 \text{ M}^{-1} \text{ cm}^{-1}$ for protein-bound label. Control experiments showed that the fluorescent labeling did not alter the inhibitory properties of the serpins.

Competition between ACT and $\alpha_1\text{PI}$ for the Binding of cat G. Cat G (0.5 μM) was reacted with buffered mixtures of fluorescently labeled ACT (5 μM) and $\alpha_1\text{PI}$ (20–75 μM). After 10 min at 25 °C, 500 μL of each reaction medium was chromatographed on a mono S HR 5/5 column (Amersham Pharmacia Biotech). Free serpins were eluted with the buffer while the cat G–serpin complexes were eluted with a mixture of buffer and 2 M NaCl. The effluent containing these complexes (total volume = 3 mL) was assayed fluorometrically using a Shimadzu RF 5000 spectrofluorimeter ($\lambda_{\text{ex}} = 495 \text{ nm}$, $\lambda_{\text{em}} = 514 \text{ nm}$ for labeled ACT; and $\lambda_{\text{ex}} = 560 \text{ nm}$, $\lambda_{\text{em}} = 580 \text{ nm}$ for labeled $\alpha_1\text{PI}$). The concentration of labeled complexes was calculated from

Scheme 1



Scheme 2



calibration curves constructed with 1:1 cat G-labeled serpin complexes dissolved in buffer containing 2 M NaCl.

RESULTS

Cat G–Serpine Binding Stoichiometry. Cat G was titrated with ACT and $\alpha_1\text{PI}$ as indicated in the Experimental Section. Both serpins gave linear titration curves which intercepted the abscissae at a molar ratio of serpin (protein concentration) to cat G (active site concentration) of 1.09 for ACT and 1.14 for $\alpha_1\text{PI}$ (data not shown). A stoichiometry of inhibition greater than unity may be interpreted to mean that a serpin behaves like a suicide inhibitor which is partly turned over like a substrate during the inhibition reaction (19). Our inhibition stoichiometries are too close to unity for such a mechanism to be valid. Our data rather suggest that the cat G–serpin binding stoichiometry is 1:1 and that our ACT and $\alpha_1\text{PI}$ preparations contain 91% and 86% of active inhibitor, respectively. These are fairly high specific activities for lyophilized proteins. The serpin concentrations indicated throughout this paper all refer to active inhibitor concentrations.

Two-Step Mechanism for the Inhibition of cat G by ACT and $\alpha_1\text{PI}$. The inhibition mechanism was investigated using the progress curve method (20–23) which consists of rapidly mixing enzyme, inhibitor, and substrate and recording the release of product (P). Under these conditions, inhibitor (I) and substrate (S) compete for the binding of enzyme (E) as illustrated in Schemes 1 or 2, where EI denotes the irreversible serpin–proteinase complex while EI* is a rapidly accumulating reversible complex whose equilibrium dissociation constant is given by $K_i^* = k_{-1}/k_1$.

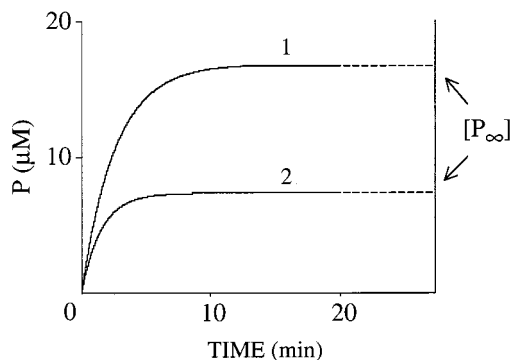


FIGURE 1: Progress curves for the cat G-catalyzed hydrolysis of 0.3 mM Suc-Ala₂-Pro-Phe-SBzl in the presence of ACT: [Cat G] = 3.2 nM, [ACT] = 0.18 μM (curve 1), or 0.4 μM (curve 2). The raw progress curves (not shown) were corrected as described previously (32) and were used to calculate the pseudo-first-order rate constant k by nonlinear regression analysis based on eq 1. $[P]$ and $[P]_{\infty}$ are the concentrations of product at any time and at infinite time, respectively.

To decide between one-step inhibition (Scheme 1) and two-step inhibition (Scheme 2), we have recorded progress curves for a wide range of inhibitor concentrations. Typical curves describing the inhibition of cat G by ACT are shown in Figure 1. These progress curves are exponentials as predicted for an irreversible inhibitor. Their asymptotic values, $[P]_{\infty}$, will be used later. Since in our experimental conditions $[I]_0 \geq 10[E]_0$ and $[P]_{\infty} \ll [S]_0$, the progress curves could be fitted by nonlinear regression analysis to the following exponential equation (23):

$$P = \frac{v_z}{k}(1 - e^{-kt}) \quad (1)$$

where k is the pseudo-first-order rate constant of inhibition, and v_z is the rate of substrate hydrolysis at $t = 0$.

Schemes 1 and 2 predict eqs 2 and 3, respectively (22, 23):

$$k = \frac{k_{\text{assoc}}[I]_0}{(1 + [S]_0/K_m)} \quad (2)$$

$$k = \frac{k_2[I]_0}{[I]_0 + K_i^*} \quad (3)$$

where $K_{i(\text{app})}^* = K_i^*(1 + [S]_0/K_m)$. Figure 2 shows that the inhibition of cat G by both ACT and α_1 PI exhibits a hyperbolic dependence of k versus $[I]_0$, indicating that it is described by eq 3 and, therefore, takes place in at least two steps. Nonlinear fits of the data of Figure 2 to eq 3 confirmed their adherence to the two-step model and gave the best estimates of k_2 and $K_{i(\text{app})}^*$. The K_m values for the cat G-catalyzed hydrolysis of Suc-Ala₂-Pro-Phe-SBzl and Suc-Ala₂-Pro-Phe-pNA were found to be 0.046 and 2.5 mM, respectively, as determined in separate experiments. These values were used to calculate K_i^* from $K_{i(\text{app})}^*$. The k_2 and K_i^* values for the two cat G-serpin pairs are compiled in Table 1, together with the calculated second-order rate constants of inhibition k_2/K_i^* .

Evidence that the EI* Complexes are Enzymatically Inactive. Scheme 2 assumes that EI* is unable to bind and turnover substrate. If EI* is partially active, k will still vary

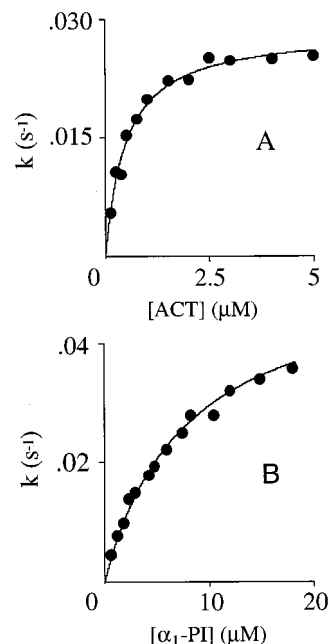


FIGURE 2: Pseudo-first-order rate constants of inhibition of cat G as a function of ACT concentration (panel A) and α_1 PI concentration (panel B). The rate constants k were measured using the progress curve method (see Figure 1). The inhibition of cat G by ACT was assessed using variable $[E]_0$, $[I]_0/[E]_0 = 15$ and 0.3 mM Suc-Ala₂-Pro-Phe-SBzl. The inhibition of cat G by α_1 PI was measured using variable $[E]_0$, $[I]_0/[E]_0 = 20$ and 10 mM Suc-Ala₂-Pro-Phe-pNA.

Table 1: Kinetic Parameters Describing the Inhibition of Cat G by ACT and α_1 PI at pH 7.4 and 25 °C^a

serpin	K_i^* (M)	k_2 (s ⁻¹)	k_2/K_i^* (M ⁻¹ s ⁻¹)
ACT	$(6.2 \pm 0.6) \times 10^{-8}$	$(2.8 \pm 0.07) \times 10^{-2}$	$(4.5 \pm 0.5) \times 10^5$
α_1 PI	$(8.1 \pm 0.9) \times 10^{-7}$	$(5.5 \pm 0.15) \times 10^{-2}$	$(6.8 \pm 0.9) \times 10^4$

^a K_i^* and k_2 were determined using the progress curve method (Figures 1 and 2).

hyperbolically with $[I]_0$ but k_2 and K_i^* will no longer have simple meanings. We therefore decided to see whether the EI* complexes are enzymatically inactive.

For a two-step inhibition process with an enzymatically inactive EI* intermediate, $[P]_{\infty}$, the amplitude of the exponential (see Figure 1) is given by (23):

$$[P]_{\infty} = \frac{k_{\text{cat}}K_i^*[E]_0[S]_0}{K_m k_2 [I]_0} \quad (4)$$

Thus, if $[P]_{\infty}$ is measured using constant concentrations of enzyme and substrate and variable concentrations of inhibitor, plots of $[P]_{\infty}$ versus $[I]_0$ should be hyperboles of the form $[P]_{\infty} = A/[I]_0$ where $A = k_{\text{cat}}K_i^*[E]_0[S]_0/K_m k_2$. Comparison of the experimental values of A with the calculated values allows one to check the inactivity of EI*.

As shown in Figure 3, both ACT and α_1 PI yield a hyperbolic dependence of $[P]_{\infty}$ with $[I]_0$. With ACT, $[P]_{\infty}$ values close to the asymptotic value of 0 could be measured which is in itself sufficient to infer that EI* is inactive. Nonlinear regression analysis showed that the data adhere to a hyperbola (see theoretical curve in Figure 3A) with $A_{(\text{experimental})} = 3.1 \times 10^{-12} \text{ M}^2$, a value that favorably compares with $A_{(\text{calculated})} = 4 \times 10^{-12} \text{ M}^2$ if allowance is

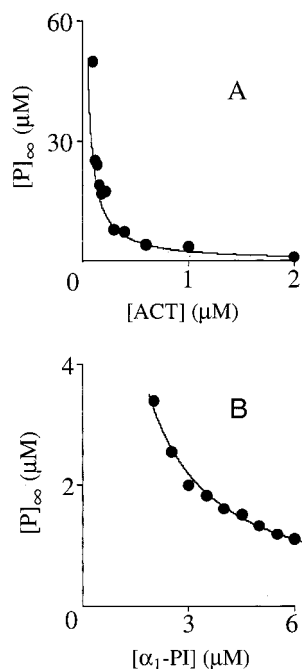


FIGURE 3: Concentration of P_{∞} as a function of inhibitor concentration. $[P]_{\infty}$, illustrated in Figure 1, was determined using the progress curve method. In the case of ACT (panel A), $[\text{cat G}] = 3.2 \text{ nM}$ and $[\text{Suc-Ala}_2\text{-Pro-Phe-SBzl}] = 0.3 \text{ mM}$. For $\alpha_1\text{PI}$ (panel B), $[\text{cat G}] = 0.16 \text{ }\mu\text{M}$ and $[\text{Suc-Ala}_2\text{-Pro-Phe-pNA}] = 3 \text{ mM}$.

made for the experimental errors on the four kinetic constants. With $\alpha_1\text{PI}$, the asymptotic value $[P]_{\infty} \rightarrow 0$ could not be approached as closely as with ACT. Nevertheless, nonlinear regression analysis gave a good fit with the model (see Figure 3B) and $A_{(\text{experimental})}$ ($6.5 \times 10^{-12} \text{ M}^2$) was sufficiently close to $A_{(\text{calculated})}$ ($9.3 \times 10^{-12} \text{ M}^2$) to conclude that this EI* complex may also be considered enzymatically inactive.

Second-Order Rate Constants for the Inhibition of cat G by ACT and $\alpha_1\text{PI}$. If $[I]_0$ is significantly lower than K_i^* , a two-step inhibition process will behave like a bimolecular reaction governed the second-order rate constant k_2/K_i^* ($E + I \xrightarrow{k_2/K_i^*} EI$). To measure k_2/K_i^* directly we have, therefore, incubated cat G with ACT or AT under the following condition: $[E]_0 = [I]_0 = 0.1K_i^*$. After selected periods of time a large excess of substrate ($[S]_0 = 6.5K_m$) was used to stop the reaction and to measure the residual enzymatic activities. Under these simplified second-order conditions, k_2/K_i^* may be calculated from eq 5:

$$\frac{v}{v_0} = \frac{1}{1 + [E]_0(k_2/K_i^*)t} \quad (5)$$

where v_0 and v are the velocities at $t = 0$ and at any time t , respectively. The data are shown in Figure 4. Nonlinear regression analysis based on eq 5 gave the best estimates of k_2/K_i^* , that is, 7×10^5 and $8.8 \times 10^4 \text{ M}^{-1} \text{ s}^{-1}$ for ACT and $\alpha_1\text{PI}$, respectively. These directly determined constants compare favorably with those calculated from k_2 and K_i^* measured by the progress curve method (Table 1).

Direct Determination of K_i^* . Progress curves characterizing two-step inhibition are described by an exponential equation (eq 1) in which v_z is the initial velocity of the

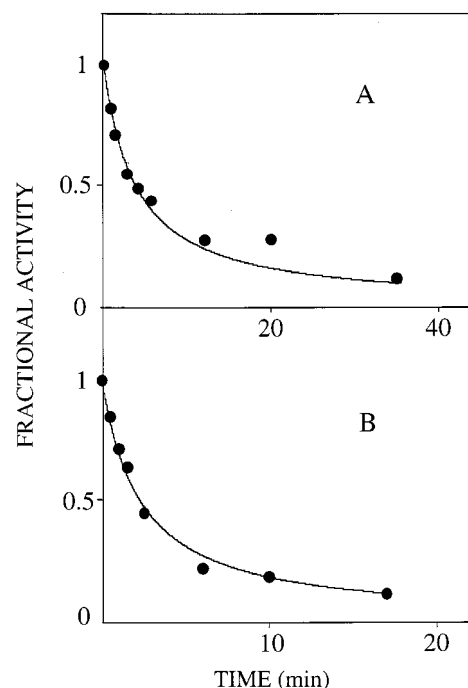


FIGURE 4: Determination of the second-order rate constants for the inhibition of cat G by ACT (panel A) and $\alpha_1\text{PI}$ (panel B). The following concentrations were used: $[\text{cat G}] = [\text{ACT}] = 6 \text{ nM}$ (panel A), $[\text{cat G}] = [\alpha_1\text{PI}] = 80 \text{ nM}$ (panel B), and $\text{Suc-Ala}_2\text{-Pro-Phe-SBzl} = 0.3 \text{ mM}$ throughout. The curves have been calculated using eq 5 and the best estimates of k_2/K_i^* determined by nonlinear regression analysis.

competitively inhibited hydrolysis of substrate (22):

$$v_z = \frac{k_{\text{cat}}[E]_0}{1 + K_m/[S]_0(1 + [I]_0/K_i^*)} \quad (6)$$

Thus, study of the dependence of v_z upon $[I]_0$ provides a means to estimate K_i^* independently. We did not use the v_z data from the progress curve analysis because one single substrate concentration was used for each inhibitor and this substrate concentration was much higher than the K_m , rendering competitive inhibition difficult to diagnose. We measured v_z in the presence of two lower substrate concentrations, $0.5K_m$ and $1.5K_m$. Significant inhibition was observed for inhibitor concentrations close to the enzyme concentrations. Under these conditions eq 6 cannot be used because it assumes that $[I]_0 \geq 10[E]_0$. We therefore employed a more general equation (16):

$$\frac{v_z}{v_0} = 1 - \frac{([E]_0 + [I]_0 + K_{i(\text{app})}^*) - \sqrt{([E]_0 + [I]_0 + K_{i(\text{app})}^*)^2 - 4[E]_0[I]_0}}{2[E]_0} \quad (7)$$

where $K_{i(\text{app})}^* = K_i^*(1 + [S]_0/K_m)$ and v_0 = velocity in the absence of inhibitor.

Figure 5 shows that the titration curves calculated using eq 7 and the best estimates of $K_{i(\text{app})}^*$ fit the experimental data fairly well. With ACT, $K_{i(\text{app})}^*$ was found to be 1×10^{-7} and $1.9 \times 10^{-7} \text{ M}$ for $[S]_0 = 0.5K_m$ and $1.5K_m$, respectively, leading to an average value of $K_i^* = 7.2 \times$

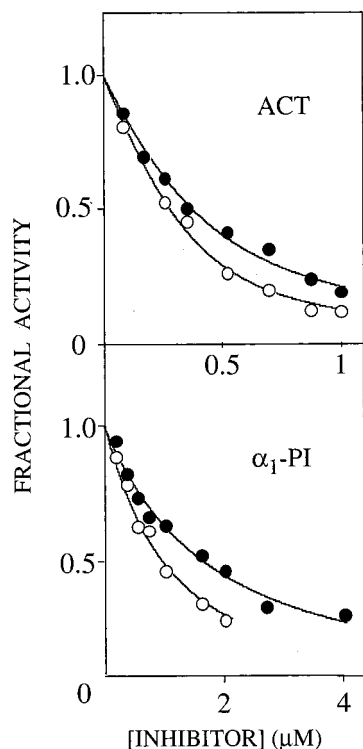


FIGURE 5: Direct determination of K_i^* for the EI^* complexes formed of cat G and ACT (upper panel) or α_1 PI (lower panel). Cat G (final concentration = $0.36 \mu\text{M}$) was added to mixtures of inhibitor and Suc-Ala₂-Pro-Phe-pNA (final concentration = 1.25 mM (○) or 3.75 mM (●)), and the release of product was recorded for a few seconds. The tangent to the progress curve at $t = 0$ was used to calculate v_z , the initial rate of substrate breakdown in the presence of inhibitor. Fractional activity = v_z/v_0 (see eq 7). The titration curves have been calculated using eq 7 and the best estimates of K_i^* (app) determined by nonlinear regression analysis.

10^{-8} M . With α_1 PI, K_i^* (app) was $8.2 \times 10^{-7} \text{ M}$ for $[S]_0 = 0.5K_m$ and $1.6 \times 10^{-6} \text{ M}$ for $[S]_0 = 1.5 K_m$, leading to $K_i^* = 5.9 \times 10^{-7} \text{ M}$. These two K_i^* values are fairly close to those measured with the progress curve method (see Table 1).

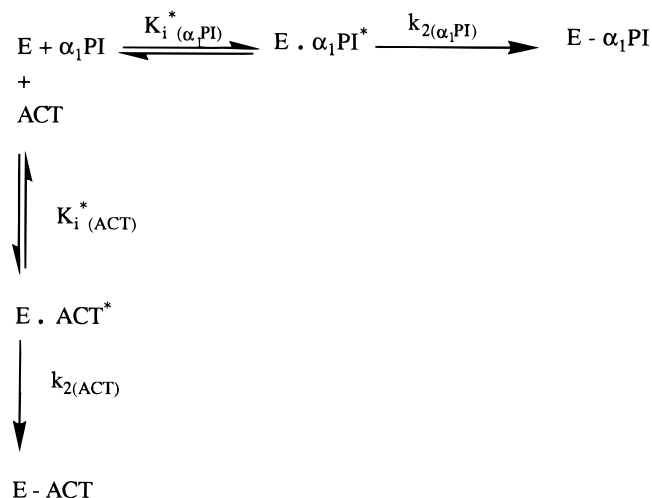
Competition between ACT and α_1 PI for the Binding of cat G. Fluorescently labeled ACT and α_1 PI were allowed to compete for the binding of cat G as illustrated in Scheme 3 in which E stands for cat G. If $[\alpha_1\text{PI}]_0 \gg [E]_0$, $[\alpha_1\text{PI}]_0 \gg K_i^*(\alpha_1\text{PI})$, $[\text{ACT}]_0 \gg [E]_0$, and $[\text{ACT}]_0 \gg K_i^*(\text{ACT})$, and if the competition mixtures are incubated long enough to allow conversion of the reaction intermediates $E \cdot \alpha_1\text{PI}^*$ and $E \cdot \text{ACT}^*$ into the final inhibitory complexes $E - \alpha_1\text{PI}$ and $E - \text{ACT}$, the concentrations of $E - \alpha_1\text{PI}$ and $E - \text{ACT}$ are related to those of the initial free serpin concentrations $[\alpha_1\text{PI}]_0$ and $[\text{ACT}]_0$ through:

$$\frac{[E - \alpha_1\text{PI}]}{[E - \text{ACT}]} = \left(\frac{k_2(\alpha_1\text{PI})}{K_i^*(\alpha_1\text{PI})} \right) \left(\frac{K_i^*(\text{ACT})}{k_2(\text{ACT})} \right) \left(\frac{[\alpha_1\text{PI}]_0}{[\text{ACT}]_0} \right) \quad (8)$$

Thus, the competition experiment provides a means to estimate the ratio of the two second-order rate constants of inhibition.

Constant concentrations of cat G were added to mixtures formed of constant concentrations of fluorescein-ACT and variable concentrations of rhodamine- α_1 PI. These concentrations were chosen in such a way that $[I]_0 \geq 25K_i^*$. After

Scheme 3



a 10 min incubation time which is long enough to allow complete conversion of the intermediates into the final inhibitory complexes, the reaction media were chromatographed on a cation exchange column (Figure 6A) which quantitatively separates free and cat G-bound serpins due to the enzyme's cationic character (Figure 6B). The concentrations of cat G- α_1 PI and cat G-ACT complexes were then assayed fluorometrically as described in the Materials and Methods section. Figure 6C shows that the molar ratio of cat G- α_1 PI to cat G-ACT is linearly related to the molar ratio of free α_1 PI to free ACT, as predicted by eq 8. The slope of the straight line, that is, the ratio of $k_2(\alpha_1\text{PI})/K_i^*(\alpha_1\text{PI})$ to $k_2(\text{ACT})/K_i^*(\text{ACT})$ was found to be 0.21, a value that favorably compares with 0.15, the ratio calculated from the constants determined by the progress curve method (Table 1), and 0.13, the ratio calculated from the directly determined second-order rate constants (Figure 4).

DISCUSSION

The activity of cat G is regulated by several protein proteinase inhibitors, namely mucus proteinase inhibitor (24) present in extravascular secretions and α_2 -macroglobulin (18), inter- α -trypsin inhibitor (25), ACT, and α_1 PI present in plasma. The α_2 -macroglobulin-proteinase complexes are partially active on substrates (18). Besides, inter- α -trypsin inhibitor forms a weak complex with cat G ($K_i = 6 \mu\text{M}$, ref 25). ACT and α_1 PI are therefore the major cat G inhibitors in plasma.

We have conclusively demonstrated that both ACT and α_1 PI inhibit cat G via a two-step reaction mechanism where the initial formation of an enzymatically inactive reversible complex EI^* is followed by an irreversible transformation of this complex into EI, the final inhibitory species. We have used the progress curve method to measure K_i^* , the equilibrium dissociation constants of the two EI^* complexes, and k_2 , the first-order rate constants for their conversion into EI. Initial velocity measurements of cat G-catalyzed hydrolyses of substrate in the presence of the two serpins permitted direct measurements of K_i^* whose values did not differ by more than 27% from those measured by the progress curve method. On the other hand, kinetics of

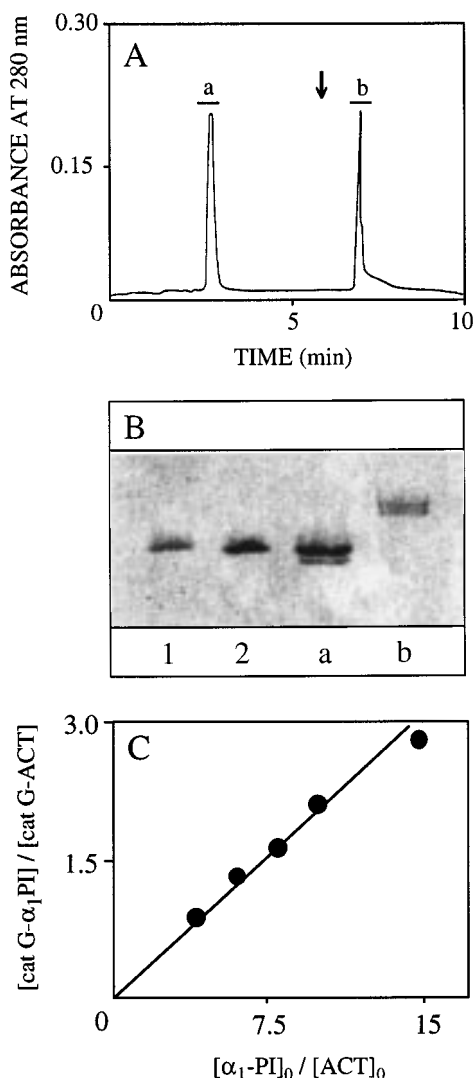


FIGURE 6: Competition between ACT and α_1 PI for the binding of cat G. (Panel A) A mixture of $0.5 \mu\text{M}$ cat G + $5 \mu\text{M}$ fluorescein-ACT + $5 \mu\text{M}$ rhodamine- α_1 PI was chromatographed as outlined in the Materials and Methods section, the arrow indicating the start of the elution with the buffer containing 2 M NaCl. (Panel B) SDS/ β -mercaptoethanol-polyacrylamide gel electrophoresis of the proteins from Peaks a and b above (lanes a and b), free ACT (lane 1), and free α_1 PI (lane 2). Comparison of the electrophoretic mobilities of the proteins contained in peaks a and b with the mobility of the free serpins indicates that peak a contains the free serpins (57 ± 4 kDa) and small amounts of cleaved serpins while peak b contains the cat G-serpin complexes (80 ± 3 kDa). (Panel C) Partition of cat G (constant concentrations) between ACT (constant concentrations) and α_1 PI (variable concentrations). The fluorescently labeled cat G-serpin complexes were isolated as shown in Panel A and assayed as outlined in the Materials and Methods section.

inhibition of cat G under conditions where $[E]_0 = [I]_0 \ll K_i^*$ allowed the direct measurement of k_2/K_i^* , the second-order rate constant of association classically referred to as k_{assoc} . The values of these two constants did not differ by more than 55% from those calculated from k_2 and K_i^* measured by the progress curve method. Last, competition between ACT and α_1 PI for the binding of cat G and assay of the final cat G-ACT and cat G- α_1 PI complexes yielded the ratio of the two second-order rate constants, a value that did not differ by more than 60% from the ratios calculated either from the progress curve method data or from the k_{assoc}

data. Our kinetic data must therefore be considered highly reliable. Previous kinetic studies on the inhibition of cat G by ACT and α_1 PI were done under second-order conditions and low enzyme and inhibitor concentrations (8, 26, 27). Under such conditions, EI^* could not be detected. However, k_{assoc} , that is, k_2/K_i^* , could be measured. Comparison of k_{assoc} from the literature with k_2/K_i^* from this paper reveals that the data reported for the cat G- α_1 PI system are all of the same order of magnitude (8, 26, 27). In contrast, k_2/K_i^* found here for the cat G-ACT pair is 2 orders of magnitude lower than the k_{assoc} reported previously (8). It is, however, close to the k_{assoc} published more recently (27).

Kinetic measurement of proteinase inhibition using a wide range of serpin concentrations provides more reliable information than second-order kinetic methods using a single serpin concentration. For instance, if a serpin-proteinase association that follows a two-step mechanism is monitored under second-order conditions using $[E]_0 \approx [I]_0 \approx K_i^*$, the resulting k_{assoc} will be apparent and underestimated because $k_{\text{assoc}} = k_2/([I]_0 + K_i^*)$ (16). Thus, to have a physical meaning, k_{assoc} should be measured using $[I]_0 < K_i^*$ so that it will be equal to k_2/K_i^* . Since K_i^* may vary from one system to another, the kinetics of inhibition should always be assessed using a wide range of $[I]_0$. The kinetic investigation will then yield either k_2/K_i^* , a reliable estimate of k_{assoc} , or k_2 and K_i^* separately.

We believe our results have pathophysiological bearing. As outlined in the first section, uncontrolled cat G-mediated proteolysis may cause severe pathological disorders. We may use our kinetic data to see whether ACT and α_1 PI play a proteolysis-preventing function in plasma. The concentrations of ACT and α_1 PI in plasma are 6 and $26 \mu\text{M}$, respectively (28, 29). Thus, the $[I]_0/K_i^*$ ratio is 100 and 32 for plasma ACT and α_1 PI, respectively. Under such conditions, the two initial $E + I \rightleftharpoons EI^*$ equilibria are almost fully shifted toward EI^* . Thus, immediately after its release in plasma, cat G will be fully taken up as EI^* complexes with ACT and α_1 PI. Calculation of its partition between the two inhibitors using a distribution diagram for multiple equilibria (30) shows that 73% binds as an EI^* complex with ACT and 27% as an EI^* complex with α_1 PI. ACT is thus the most prominent inhibitor from this point of view. On the other hand, we have shown that both EI^* complexes are enzymatically inactive. Thus, in plasma, the two serpins behave like tight-binding reversible inhibitors of cat G whose inhibitory potential does not depend on the formation of the stable inhibitory species EI characteristic of serpins.

Since inhibition must also be fast to be efficient *in vivo* (15) we have tentatively calculated k^* the rate constant of EI^* formation: $k^* = k_1[I]_0 + k_{-1}$ which may also be written as $k^* = k_{-1}(1 + [I]_0/K_i^*)$. Since accumulation of EI^* requires $k_{-1} \gg k_2$, one gets $k^* \gg k_2(1 + [I]_0/K_i^*)$. This leads to $k^*_{(\text{ACT})} \gg 2.8 \text{ s}^{-1}$ ($t_{1/2} \ll 0.25 \text{ s}$) and $k^*_{(\alpha_1\text{PI})} \gg 1.8 \text{ s}^{-1}$ ($t_{1/2} \ll 0.4 \text{ s}$). Thus, both EI^* complexes form very rapidly and at rates strongly suggesting physiological inhibitory function (15).

The present results lead to the general conclusion that any serpin that inhibits a target proteinase via a two-step mechanism will express its inhibitory power as an EI^* complex if its *in vivo* concentration is significantly higher than K_i^* and if EI^* is inactive. For such serpins the $EI^* \xrightarrow{k_2} EI$

conversion will mainly serve to change the conformation of the inhibitor so as to ensure its rapid plasma elimination (31). In short, inhibition will be governed by K_i^* while plasma elimination will depend on k_2 .

ACKNOWLEDGMENT

We thank Dr. Jean-Luc Dimicoli, INSERM U 350, Orsay, France, for mathematical advice.

REFERENCES

- Hof, P., Mayr, I., Huber, R., Korzus, E., Potempa, J., Travis, J., Powers, J. C., and Bode, W. (1996) *EMBO J.* 15, 5481–5491.
- Powers, J., Kam, C., Narasimhan, L., Oleksyszyn, J., Hernandez, M., and Ueda, T. (1989) *J. Cell Biol.* 39, 33–46.
- Bieth, J. G. (1986) in *Regulation of Matrix Accumulation* (Mecham, R. P., Ed.) pp 217–320, Academic Press, New York.
- Wintroub, B., Klickstein, L., Dzau, V., and Watt, K. (1984) *Biochemistry* 23, 227–232.
- Pratt, C., Tobin, R., and Church, F. (1990) *J. Biol. Chem.* 265, 6092–6097.
- Ferrer-Lopez, P., Renesto, P., Schattner, M., Bassot, S., Laurent, P., and M., C. (1990) *Am. J. Physiol.* 258, C1100–C1107.
- Huber, R., and Carrell, R. W. (1989) *Biochemistry* 28, 8951–8966.
- Beatty, K., Bieth, J. G., and Travis, J. (1980) *J. Biol. Chem.* 255, 3931–3934.
- Potempa, J., Korzus, E., and Travis, J. (1994) *J. Biol. Chem.* 269, 15957–15960.
- Lawrence, D. A., Ginsburg, D., Day, D. E., Berkenpas, M. B., Verhamme, I. M., Kvassman, J.-O., and Shore, J. D. (1995) *J. Biol. Chem.* 270, 25309–25312.
- Wilczynska, M., Fa, M., Ohlsson, P.-I., and Ny, T. (1995) *J. Biol. Chem.* 270, 29652–29655.
- Travis, J., Bowen, J., and Baugh, R. (1978) *Biochemistry* 17, 5651–5656.
- Schechter, N., Sprows, J., Schoenberger, O., Lazarus, G., Cooperman, B., and Rubin, H. (1989) *J. Biol. Chem.* 264, 21308–21315.
- Davril, M., Laine, A., and Hayem, A. (1987) *Biochem. J.* 245, 699–704.
- Bieth, J. G. (1984) *Biochem. Med.* 32, 387–397.
- Bieth, J. G. (1995) *Methods Enzymol.* 248, 59–84.
- Ermoloeff, J., Boudier, C., Laine, A., Meyer, B., and Bieth, J. G. (1994) *J. Biol. Chem.* 269, 29502–29508.
- Travis, J., and Salvesen, G. S. (1983) *Annu. Rev. Biochem.* 52, 655–709.
- Wright, H. T., and Scarsdale, J. N. (1995) *Proteins: Struct. Funct. Genet.* 22, 210–225.
- Cha, S. (1975) *Biochem. Pharmacol.* 24, 2177–2185.
- Morrison, J. F. (1982) *Trends Biochem. Sci.* 61, 201–301.
- Morrison, J. F., and Walsh, C. T. (1988) *Adv. Enzymol. Relat. Areas Mol. Biol.* 61, 201–301.
- Tian, W.-X., and Tsou, C.-L. (1982) *Biochemistry* 21, 1028–1032.
- Thompson, R. C., and Ohlsson, K. (1986) *Proc. Natl. Acad. Sci. U.S.A.* 83, 6692–6696.
- Potempa, J., Kwon, K., Chawla, R., and Travis J. (1989) *J. Biol. Chem.* 264, 15109–15114.
- Travis, J., Owen, M., George, P., Carrell, R., Rosenberg, S., Hallwell, R. A., and Barr, P. J. (1985) *J. Biol. Chem.* 260, 4384–4389.
- Lomas, D. A., Stone, S. T., Llewellyn-Jones, C., Koegan, M. T., Wang, Z. M., Rubin, H., Carrell, R. W., and Stockley, R. A. (1995) *J. Biol. Chem.* 270, 23437–23443.
- Jeppsson, J. O., Laurel, C. B., and Fagerhol, M. K. (1978) *Eur. J. Biochem.* 83, 143–153.
- Laurell, C. B., and Jeppsson, J. O. (1975) in *Plasma: The plasma proteins, Structure, Function, and Genetic Control* (Putnam, F. W., Ed.) pp 229–264, Academic Press, New York.
- Stefano, C., Princi, P., Rigano, C., and Sammartano, S. (1988) *Ann. Chim.* 78, 55–82.
- Mast, A. E., Enghild, J. J., Pizzo, S. V., and Salvesen, G. (1991) *Biochemistry* 30, 1723–1730.
- Faller, B., Cadène, M., and Bieth, J. G. (1993) *Biochemistry* 32, 9230–9235.

BI980223Q